Since January 2020 Elsevier has created a COVID-19 resource centre with free information in English and Mandarin on the novel coronavirus COVID-19. The COVID-19 resource centre is hosted on Elsevier Connect, the company's public news and information website.

Materials Science and Engineering C 76 (2017) 735–742

Contents lists available at ScienceDirect

Materials Science and Engineering C

journal homepage: www.elsevier.com/locate/msec

Biopolymeric nano/microspheres for selective and reversible adsorption of coronaviruses

Justyna Ciejka [a,b], Karol Wolski [b], Maria Nowakowska [b], Krzysztof Pyrc [a,c,*], Krzysztof Szczubiałka [b,*]

[a] Laboratory of Virology, Malopolska Centre of Biotechnology, Jagiellonian University, Gronostajowa 7a, 30-387 Krakow, Poland
[b] Faculty of Chemistry, Jagiellonian University, Ingardena 3, 30-060 Krakow, Poland
[c] Microbiology Department, Faculty of Biochemistry, Biophysics and Biotechnology, Jagiellonian University, Gronostajowa 7, 30-387 Krakow, Poland

ARTICLE INFO

Article history:
Received 3 November 2016
Received in revised form 9 February 2017
Accepted 4 March 2017
Available online 6 March 2017

Keywords:
Coronavirus
Adsorbent
Chitosan
Genipin
Nanospheres
Microspheres
Adsorption
Virus titration
Cytopathic effect
Polymerase chain reaction

ABSTRACT

A novel biopolymeric material in the form of nano/microspheres was developed which was capable of adsorbing coronaviruses. The biopolymer was obtained by crosslinking of chitosan (CHIT) with genipin, a nontoxic compound of plant origin, in inverted emulsion and reacting the chitosan nano/microspheres obtained (CHIT-NS/MS) with glycidyltrimethyl-ammonium chloride (GTMAC). As a result the nano/microspheres of N-(2-hydroxypropyl)-3-trimethyl chitosan (HTCC-NS/MS) were obtained. HTCC-NS/MS were studied as the adsorbents of human coronavirus NL63 (HCoV-NL63), mouse hepatitis virus (MHV), and human coronavirus HCoV-OC43 particles in aqueous virus suspensions. By studying cytopathic effect (CPE) caused by these viruses and performing PCR analyses it was found HTCC-NS/MS strongly adsorb the particles of HCoV-NL63 virus, moderately adsorb mouse hepatitis virus (MHV) particles, but do not adsorb HCoV-OC43 coronavirus. The adsorption capacity of HTCC-NS/MS well correlated with the antiviral activity of soluble HTCC against a given virus. Importantly, it was shown that HCoV-NL63 particles could be desorbed from the HTCC-NS/MS surface with a salt solution of high ionic strength with retention of virus virulence. The obtained material may be applied for the removal of coronaviruses, purification and concentration of virus samples obtained from biological matrices and for purification of water from pathogenic coronaviruses.

1. Introduction

The multistep procedures of virus separation, concentration and purification are of great importance for the preparation of the products containing a virus as the principal component, such as cell culture-derived virus stocks for vaccine manufacturing, research and gene therapy [1–4]. On the other hand, virus separation is also required during procedures involving virus removal such as preparation of biopharmaceutical products, which should be free of any viral contamination [5] and in the purification of drinking water from water-borne viruses such as hepatitis A virus, hepatitis E virus, norovirus, rotavirus, and adenovirus [6].

Typical virus separation methods encompass membrane filtration [7] including tangential flow filtration [8], ultracentrifugation [9], electrophoresis [10,11], agglutination [12], and chromatography [13]. However, they are often expensive (cost of the purification may constitute up to 80% of the total cost (14)), time- and labor-consuming and difficult to scale-up.

An alternative method of virus purification/removal is virus adsorption which takes advantage of the attractive interaction between a virion and an adsorbent. Such interaction may be of various nature. Since the surface of viruses may become charged depending on their isoelectric point (IEP) and pH of the environment, their interactions with the adsorbents may be primarily electrostatic (at pH values sufficiently different from IEP) or mostly hydrophobic (at pH ≈ IEP) [15]. The surface of virions may be both positively (at pH < IEP) and negatively (at pH > IEP) charged so they may be adsorbed by sorbents with both negatively and positively charged surface, respectively. Consequently, materials previously reported as virus adsorbents are of different nature. The examples of inorganic adsorbents are clays such as kaolinite, montmorillonite, and bentonite [16]. Their adsorption efficiency for viruses is very different but generally low. For kaolinite at the concentration of 50 g/l the log removal value (LRV) was 2.18, while montmorillonite and bentonite were much less efficient. Thermodynamic studies indicated that the adsorption of some bacteriophages to clays depended on the hydrophobicity of the surface of both clays and viruses

* Corresponding authors at: Microbiology Department, Faculty of Biochemistry Biophysics and Biotechnology, Jagiellonian University, Gronostajowa 7, 30-387 Krakow, Poland.
E-mail addresses: k.a.pyrc@uj.edu.pl (K. Pyrc), szczubia@chemia.uj.edu.pl (K. Szczubiałka).

http://dx.doi.org/10.1016/j.msec.2017.03.047
0928-4931/

[17]. The ability to adsorb viruses was shown for hybrid organic-inorganic materials, e.g., cellulose nanofibers enriched with α-Fe_2O_3 nanoparticles [18]. The hybrid inorganic nanoparticles with virus particles covalently bound to their surface have been also reported and used as virus delivery systems [19].

Most of the organic adsorbents used for virus separation studied so far have been (modified) natural polymers, both neutral and charged, but synthetic polymers such as polystyrene substituted with arginine [20] have been also reported. Polymers used as adsorbents are mainly polysaccharides. The examples of polysaccharide adsorbents include anionic sulfated polysaccharides such as heparin [13], rhamnan [21], and fucan [22], and cationic chitosan. Polymeric membranes formed from chitosan and polyvinyl alcohol nanofibres cross-linked with glutaraldehyde have the ability to adsorb porcine parvovirus (PPV) and sindbis virus (SINV) particles [23,24]. Influenza A virus particles may be adsorbed by the carbohydrate-functionalized chitosan filaments [25]. The application of proteins and peptides as adsorbents has been also reported [26,27].

Adsorbents for various viruses have been described including alfaherpesviruses (pseudorabies virus (PrV) and bovine herpesvirus 1 (BHV-1) [28]), influenza A virus [25], porcine parvovirus (PPV) [26], sindbis virus (SINV) [25], retroviruses [13], poliovirus [29], and foamy virus [8]. Importantly, the only adsorbent for coronaviruses that has been tested so far, based on clay minerals, could adsorb bovine coronavirus. The adsorption was irreversible, making the adsorbent useless for aforementioned applications [30].

In our previous study we demonstrated that a chitosan derivative, i.e., (N-(2-hydroxypropyl)-3-trimethyl chitosan (HTCC)) shows anticoronaviral properties [31]. The polymer showed high specificity towards coronaviruses, as it inhibited replication of coronaviruses that belong to two separate genera: HCoV-NL63 (alphacoronavirus) and the mouse hepatitis virus (MHV; betacoronavirus). Further study proved that fine-tuning of HTCC substitution degree enables it to inhibit replication of all human coronaviruses [32].

Study on the mechanism of action showed that the polymer interacts with the S protein of HCoV-NL63 and forms a protein-polymer complex, which results in virus neutralization. Although neutralized virions retained the ability to bind to the attachment receptor (heparan sulfate proteoglycans), their interaction with the actual fusion receptor was blocked [33]. Others also reported that HTCC may be used in the form of electrospun HTCC-PVA fibers to adsorb porcine parvovirus (PPV) and sindbis virus (SINV) [23].

The aim of our present study was to exploit high affinity of HTCC to the S protein of coronaviruses and to obtain a convenient adsorbent for isolation and/or removal of coronaviruses form biological matrices for research purposes and for removal of coronaviruses from water. For this purpose chitosan nano/microspheres (CHIT-NS/MS) crosslinked with genipin, a natural compound obtained from the fruit of *Gardenia jasminoides*, were prepared and then cationized with GTMAC to obtain nano/microspheres of HTCC (HTCC-NS/MS). Chemical composition of obtained biomaterials was investigated using elemental analysis (EA) and spectroscopic methods. The morphology and size of the polymeric objects obtained was visualized using microscopic techniques, i.e., confocal microscopy and transmission electron microscopy (TEM). The hydrodynamic radius of the nanospheres was determined using dynamic light scattering (DLS) technique. Surface charge in different media was assessed using zeta potential measurements. The ability of the biomaterial to adsorb selected coronaviruses (HCoV-NL63, MHV and HCoV-OC43) was assessed. Changes in the infectivity of viral samples, due to interaction with adsorbent, were evaluated by virus titration according to Reed and Muench method and compared with total amount of viral RNA copies using real time PCR analysis. Adsorption and desorption of coronaviral particles on/from the surface of HTCC-NS/MS was directly visualized using atomic force microscopy (AFM) technique. Careful optimization of the material allowed for recovery (desorption) of infective coronaviral particles, which further broadens its possible applications. An advantage of the studied material is that chitosan (used in many other virus-related applications involving antiviral materials [34] and antiviral drugs [35,36]) and genipin, are both non-toxic substances.

2. Materials and methods

2.1. Materials

Chitosan (CHIT, low molecular weight, 75–85% deacetylated, Sigma-Aldrich), genipin (98%, Challenge Bioproducts), sorbitan monopalmitate (Span®40, Sigma-Aldrich), sorbitan monooleate (Span®80, Sigma-Aldrich), glycidyltrimethylammonium chloride (GTMAC, ≥90%, Sigma-Aldrich), cyclohexane (p.a, POCh), glacial acetic acid (CH_3COOH, 99,85% pure p.a., CHEMPUR), acetone (POCh), methanol (POCh) and sodium chloride (NaCl, POCh) were used as received. Doubly distilled water was deionized using the Millipore Simplicity system.

2.2. Preparation of CHIT-NS/MS and functionalization of their surface

In order to obtain the polymer material in the form of nano/microspheres previously described method was used [37]. The method is based on cross-linking of chitosan in an inverted emulsion with genipin, a non-toxic cross-linking agent. In view of the need to obtain the objects of the smallest size, the synthesis was performed in an ultrasonic bath at the stage of chitosan cross-linking.

In the first step of the synthesis, 0.5 g of Span 40 and 0.26 ml of Span 80 were dissolved in 200 ml of cyclohexane. Then, 35 ml of 2% (w/w) chitosan solution dissolved in 2% (v/v) acetic acid was added. The mixture was stirred with a mechanical stirrer at 1200 rpm and a reversed emulsion was formed. Then, the emulsion was placed in an ultrasonic bath and sonicated for 15 min to further reduce the size of the droplets in the emulsion. To sonicated emulsion 1 ml of 5% (w/v) ethanol solution of genipin was added dropwise. The sonication was continued in pulsed mode for approximately 8 h at 40 °C until a blue color appeared. The dispersion was left for 12 h in the dark. After completion of the crosslinking process the supernatant was decanted and the polymer material was washed thrice with cyclohexane. The nano/microspheres crosslinked with genipin (CHIT-NS/MS) were separated by centrifugation at 10,600 rcf for 15 min and washed thrice with cyclohexane. Finally, CHIT-NS/MS were washed with methanol, concentrated by partial drying and used in the subsequent synthesis steps.

The surface of CHIT-NS/MS was cationically modified using glicydyltrimethylammonium chloride (GTMAC). Briefly, the material obtained in the first step of the synthesis was separated into four equal parts. One of them was left as reference material (CHIT-NS/MS), and three other parts were used for synthesis of cationically modified chitosan nano/microspheres (HTCC-NS/MS). In order to obtain material with three different degree of substitution, the synthesis was carried out at 57 °C for 6, 24 and 48 h yielding the chitosan hydrogel with low, medium and high degree of surface modification (L HTCC-NS/MS, M-HTCC-NS/MS, and H-HTCC-NS/MS, respectively). Obtained materials were separated by centrifugation at 10,600 rcf for 15 min and purified by washing with distilled water until conductivity of the flow through was close to the conductivity of distilled water. At no stage of the purification process the material was allowed to dry completely. The adsorbent obtained was stored in distilled water before using in biological studies.

2.3. Physicochemical characterization of CHIT-NS/MS

Elemental analysis (C, H, and N) was performed with an EuroEA 3000 Elemental analyzer and IR spectra were recorded using dried samples at room temperature on a Nicolet IR200FT-IR spectrophotometer equipped with an ATR accessory. In both cases, solvent was removed by freeze-drying. Dynamic light scattering (DLS) and zeta potential

measurements were performed with Malvern Nano ZS light scattering apparatus (Malvern Instrument, Worcestershire, UK) using 633 nm laser light. The intensity of the scattered light was measured by the avalanche photodiode at an angle of 173°. The zeta potential of the polymeric NS/MS was measured using the technique of laser Doppler velocimetry. The measurement of each sample was performed five times at concentration of 1 mg/ml in distilled water (z-averaged hydrodynamic diameters (dz), dispersity index (DI) and zeta potential (ζ)), and in the cell culture medium (3% H&E) (ζ only). The distribution profiles of dz., DI and ζ of the samples were calculated using the software provided by the manufacturer.

2.4. Microscopic characterization of CHIT-NS/MS and x-HTCC-NS/MS

2.4.1. TEM microscopy

Transmission electron microscopy (TEM JEOL JEM-2100) was used to visualize CHIT-NS/MS and HTCC-NS/MS. The dispersion of hydrogel adsorbent was sonicated for 5 min and 5 μl of the sample was applied to an electron microscopy copper grid (Cu 200 mesh Formvar/Carbon) and incubated for 30 min. An excess of the solution was removed with tissue paper. The images were recorded at 200 kV.

2.4.2. Confocal microscopy

The samples of hydrogel adsorbent were visualized using optical microscope Ti-E Nikon with A1Si confocal system. 10 μl of suspension of CHIT-NS/MS or HTCC-NS/MS was placed on the glass slide and covered with coverslip. Since chitosan cross-linked with genipin is fluorescent, there was no need to use a fluorescence-label. 561 nm diode laser was used to excite the sample.

2.4.3. Atomic force microscopy (AFM)

The topography of the surface of hydrogel adsorbent was measured using a Dimension Icon AFM (Bruker, Santa Barbara, CA) microscope. The measurements were performed in semi-contact tapping mode (PeakForce Tapping (PFT) and QNM®) using standard silicon cantilevers (elastic constant of 0.4 N/m and 2 nm blade diameter). The samples were dried under nitrogen and the measurements were performed in air. All measurements were carried out with low downforce so as not to damage the delicate surface of the hydrogel.

Silicon wafers were cleaned by immersion in freshly prepared "piranha" solution, i.e., a mixture of 30% hydrogen peroxide and of 98% sulfuric acid (VI) mixed at 1:3 volume ratio. After 30 min, etched plates were washed exhaustively with distilled water and dried under argon before deposition of the tested materials.

10 μl of the suspension of the adsorbents was taken during the experiment, i.e., after 30 min adsorption step and the desorption step and applied on a silicon wafer. The samples were then incubated for 30 min at room temperature. The excess of the sample was removed by rinsing three times with 500 μl of filtered PBS. Subsequently, samples were fixed for 30 min using 3% glutaraldehyde solution in PBS at room temperature. Fixative was removed and the samples were washed five times with 500 μl of distilled water. The samples were stored in distilled water at 4 °C. Before measurements the samples were dried under argon.

2.5. Cell cultures

Macaca mulatta kidney epithelial cell line (LLC-MK2) (ATCC: CCL-7 cell line) was maintained in minimal essential medium (MEM) containing 2 parts of Hank's MEM and 1 part of Earle's MEM (PAA Laboratories) supplemented with 3% heat-inactivated fetal bovine serum (PAA Laboratories), penicillin (100 U/ml), and streptomycin (100 μg/ml) (3% H&E). Murine L cells stably transfected with the N-Ceacam receptor (LR7) were maintained in Dulbecco-modified Eagle's medium (DMEM) (PAA Laboratories) supplemented with 3% heat-inactivated fetal bovine serum (PAA Laboratories), penicillin (100 U/ml), streptomycin (100 μg/ml), and G418 (50 μg/ml, Sigma-Aldrich) (3% DMEM). Human colon carcinoma cell line (HCT-8) (ATCC: CCL-244) was maintained in RPMI-1640 medium supplemented with 3% heat-inactivated fetal bovine serum (PAA Laboratories), penicillin (100 U/ml), and streptomycin (100 μg/ml) (i.e., 3% RPMI). Cells were cultured on T25 flasks (TPP) at 37 °C with 5% CO_2 and 95% humidity. For cell maintenance and storage cell culture media were additionally supplemented with ciprofloxacin (5 μg/ml).

2.6. Virus preparation, infection and titration

Human coronavirus NL63 (HCoV-NL63), human coronavirus OC43 (HCoV-OC43) and murine hepatitis virus (MHV strain A59) were propagated by infecting LLC-MK2, HCT 8 and LR7 cells, respectively. The cells were infected and incubated at 32 °C (HCoV NL63, HCoV OC43) or 37 °C (MHV) in atmosphere containing 5% CO_2 until appearance of the cytopathic effect (CPE), i.e., for 6 days (HCoV NL63, HCoV OC43) or 2 days (MHV) post-infection. The samples were lysed by two freeze-thaw cycles and stored at −80 °C. Control samples from mock infected cells (LLC-MK2, HCT-8, LR7) were prepared and stored in the same manner.

Virus yield was determined by virus titration on fully confluent cells seeded on 96 well plates, according to Reed and Muench formula [38]. The LLC-MK2 and HCT-8 cells were incubated at 32 °C for 6 days (HCoV NL63 and HCoV OC43 respectively), and LR7 cells at 37 °C for 2 days (MHV). CPE was scored using an inverted microscope.

2.7. Isolation of viral nucleic acid and detection by reverse transcription and quantitative real-time PCR

Viral RNA was isolated from the cell culture supernatants using EZ-10 Spin Column Total RNA Mini-Preps super kit (Bio Basic Canada Inc., Canada) according to the manufacturer's instructions. Reverse transcription was carried out using a high-capacity cDNA reverse transcription kit (Thermo Scientific, Poland) according to the manufacturer's instructions. Virus yield was determined using real-time PCR. Briefly, 2.5 μl of cDNA was amplified in 10 μl reaction mixture containing 1 × TaqMan® Universal PCR Master Mix, No AmpErase®UNG (Applied Biosystems, USA), specific probe (200 nM) labeled with FAM (6 carboxyfluorescein) and TAMRA (6 carboxytetramethylrhodamine) and primers (900 mM). Rox was used as a reference dye. The sense primer [63NF2] was: 5′ AAA CCT CGT TGG AAg CGT GT 3′. The antisense primer [63NR1] was: 5′ CTG TGG AAA ACC TTT GGC ATC 3′. The probe [63NP] was: FAM-ATG TTA TTC AGT GCT TTG GTC CTC GTG AT-TAMRA. The reaction was carried out using a 7500 fast real-time PCR machine (Applied Biosystems, USA) with the following steps: 2 min at 50 °C, 10 min at 95 °C and 40 cycles of 15 s at 95 °C, and 1 min at 60 °C.

2.8. Adsorption/desorption of the viral particles on/from the surface of the adsorbents

The HTCC-NS/MS samples were washed thrice with cell culture medium (3% H&E) and centrifuged at 16,000 rcf for 10 min. The wet samples of HTCC-NS/MS were used for further testing. Briefly, 80 μl of the infected or mock-infected cell lysate was added to 420 μl of sample containing 5 mg HTCC-NS/MS in 3% H&E. To enable uniform adsorption of virions, samples were mixed at 1200 rpm for 30 min at 23 °C. After the incubation adsorbents were centrifuged at 16,000 rcf for 5 min. The supernatants were collected and the quantity of infectious virus particles was assessed with titration. Further, the quantity of viral RNA per sample was evaluated with RT-qPCR. Control samples (i.e., containing no adsorbent) were prepared in the same manner. In the next step, pelleted adsorbents were washed five times with PBS to remove excess of the viral particles which were not bound to the surface of HTCC-NS/MS. After the last cycle of washing supernatants were collected and virus was quantified by titration and RT-qPCR.

To desorb viral particles from the surface of HTCC-NS/MS, 500 μl of 2 M NaCl was added to each sample. Samples were mixed for 30 min at 1200 rpm at 23 °C. Subsequently, 10 μl samples of the adsorbents were centrifuged at 16,000 rcf for 5 min. Virus was quantified in supernatants by titration and RT qPCR.

The influence of 2 M NaCl on virus infectivity was evaluated. For this purpose 80 μl of viral suspension was incubated at 23 °C throughout the duration of the experiment. Finally, 500 μl of 2 M NaCl or PBS was added to the samples. The samples were mixed for 30 min at 1200 rpm at 23 °C, and the virus was quantified by titration and RT qPCR.

Table 1
Zeta potential of chitosan nanospheres (CHIT-NS) and cationically modified nanospheres with (L-HTCC-NS, M-HTCC-NS, and H-HTCC-NS) in deionized water and 3% H&E.

Particles	Zeta potential ζ [mV]	
	Water	3% H&E
–	–	−7.2 ± 0.5
CHIT-NS	+9.9 ± 0.7	−3.3 ± 0.2
L-HTCC-NS	+33.3 ± 2.4	+5.2 ± 2.1
M-HTCC-NS	+34.3 ± 1.5	+7.4 ± 1.0
H-HTCC-NS	+36.1 ± 1.9	+7.7 ± 0.6

3. Results and discussion

3.1. Physicochemical characterization of CHIT-NS/MS

CHIT-NS/MS used in this study were synthesized by cross-linking of chitosan (CHIT) with genipin according to the method previously described [37], modified by performing the synthesis in an ultrasonic bath to decrease the size of the microspheres, thereby increasing their surface area/mass ratio and improving their sorptive properties. The obtained particles were disperse in size, ranging from tens of nanometers to micrometers. The average size of the micrometer-sized fraction, as determined with confocal laser scanning microscopy and TEM (Fig. 1) was ~2.5 μm ranging from 0.3 to 12.3 μm.

The surface of CHIT-NS/MS was then cationized using glycidyltrimethylammonium chloride (GTMAC) whose glycidyl groups reacted with the primary amino groups of chitosan [31,39] yielding HTCC-NS/MS. The cationic modification of CHIT-NS/MS was confirmed with FTIR-ATR spectroscopy (see Fig. A1 in Supplementary Information) and elemental analysis (see Table A1 in Supplementary Information). By changing the substitution reaction time the cationically modified particles were obtained with three different degrees of substitution (DS) with GTMAC (corresponding to different cationic charge density), and marked as L-HTCC-NS/MS, M-HTCC-NS/MS, and H-HTCC-NS/MS for particles with low, medium and high DS, respectively. It was confirmed that the cationic functionalization of the CHIT-NS/MS particles did not significantly change their size, as found from confocal microscopy and DLS measurements (see Table A2 in Supplementary Information). To obtain a nanometer-sized fraction the synthesized particles were filtered using a syringe filter with a pore diameter of 0.22 μm. This allowed isolation of a particle fraction with an average diameter of 60 nm, as found from the DLS measurements. The respective nanoparticles were marked as CHIT-NS, L-HTCC-NS, M-HTCC-NS, and H-HTCC-NS. The measurements of the zeta potential of the nanospheric fraction of the particles were performed in water and in 3% H&E (Table 1).

The data presented in Table 1 indicate that the positive zeta potential of CHIT-NS significantly increased due to cationic modification with GTMAC. The values of the zeta potential increase in the sequence CHIT-NS < L-HTCC-NS < M-HTCC-NS < H HTCC-NS in agreement with increasing degree of substitution of the particle surface. The values of the zeta potential for all three types of HTCC-NS in water are higher than +30 mV, implying that they are able to form stable aqueous suspensions. The zeta potential of HTCC-NS in 3% H&E is much lower, probably due to binding negatively charged serum proteins [40].

3.2. HCoV-NL63 adsorption on H-HTCC-NS/MS particles

At the first stage, adsorption of the HCoV-NL63 virus to the NS/MS was evaluated. Briefly, 5 mg of H-HTCC-NS/MS was mixed with the virus suspension ($TCID_{50}$ = 1,700,000 per ml) and incubated at 23 °C for 30 min with mixing. A viral suspension ((7.8 ± 0.7) · 106 RNA copies per ml) without H-HTCC-NS/MS was used as a control (Fig. 2). H-HTCC-NS/MS were subsequently removed by centrifugation, and the virus yield was compared to that of the reference sample incubated without H-HTCC-NS/MS. RT-qPCR analysis revealed the decrease by (7.2 ± 0.8) × 106 copies/ml, i.e., 92% of virions (Fig. 2). Yet, one may speculate that the decrease may result simply from virion/RNA degradation.

It was then checked if the viral particles could be desorbed from H-HTCC-NS/MS surface by increasing the ionic strength of the solution. NS/MS were first washed with 0.25 M NaCl or with 2.0 M NaCl. Washing the particles with a 0.25 M NaCl solution resulted in only a slight virus desorption, while using a 2.0 M NaCl solution allowed significant virus recovery, i.e. (2.4 ± 0.9) · 10^6 copies/ml, which constituted 34% of the adsorbed virus particles. The enhancement in the recovery of virus particles resulting from the increased ionic strength implies that the virus-polymer interaction is of electrostatic nature [41].

Even though obtained results were promising, they only prove presence of viral nucleic acids and not the presence of infectious virus particles. Obviously, such an increase in ionic strength may affect virus integrity and hamper its infectivity, as previously reported for some other viral species. To make an example, elution of adsorbed retrovirus with 1 M NaCl resulted in 50% loss of infectivity due to envelope damage [13]. Yet, analysis performed for HCoV-NL63 revealed that incubation of

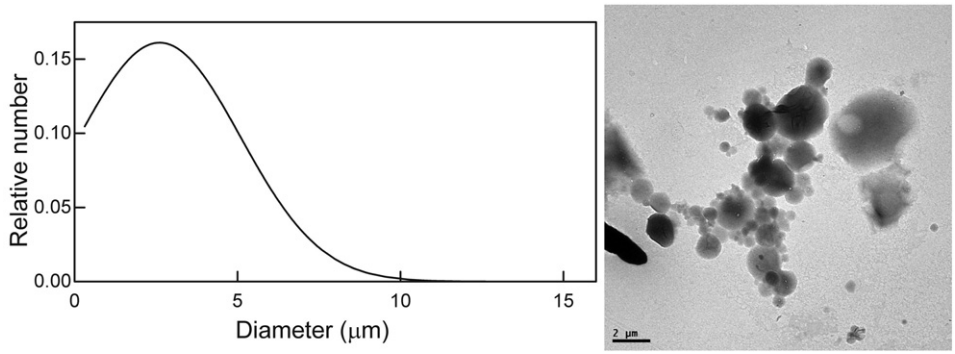

Fig. 1. The size distribution of the particles obtained from the confocal microscopy (left) and a TEM image of CHIT-NS/MS (right).

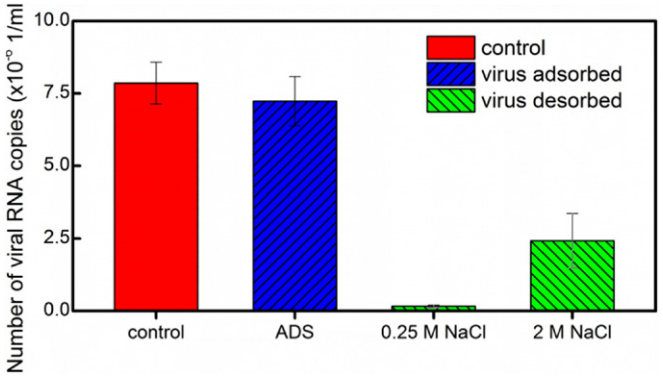

Fig. 2. The number of free HCoV-NL63 RNA copies in the virus suspension before addition of H-HTCC-NS/MS (control), the number of viral RNA copies adsorbed on H-HTCC-NS/MS (ADS) and the number of viral RNA copies desorbed from H-HTCC-NS/MS in 0.25 and 2.0 M NaCl. All experiments were repeated thrice and values are presented as an average ± SD.

virions in 2 M NaCl solution did not result in infectivity decrease compared to the PBS solution, as determined by virus titration and RT-qPCR (data not shown).

3.3. Mapping of HTCC-NS/MS surface after incubation with viral particles

Even though already earlier experiments suggested that HTCC-NS/MS are able to adsorb coronaviral particles, which subsequently may be recovered without the loss of infectivity, a direct method was used to confirm this finding. The atomic force microscopy (AFM) is a technique, which allows for surface mapping with resolution allowing for visualization of individual virions. Lysate of HCoV-NL63-infected (virus sample) and mock-infected (control sample) cells were incubated with H-HTCC-NS/MS for 30 min at 23 °C in 3%H&E. Subsequently, H-HTCC-NS/MS pellets were washed with PBS and in final step incubated in 2 M NaCl. AFM images were captured for H-HTCC-MS deposited on silica wafer (Fig. 3).

Obtained images clearly show that the surface of H-HTCC-NS/MS incubated with the control sample is smooth (Fig. 3A), in contrast to the surface of H-HTCC-NS/MS incubated with virus-containing solution (Fig. 3B). On the latter one, densely distributed spherical objects with diameter of ~140 nm may be observed, which corresponds roughly to the coronavirus size [42]. Larger object ~285 nm in diameter was also observed, but it may be attributed to HCoV-NL63 virion aggregate. Further, H-HTCC-NS/MS particles were stripped off the bound virus using 2 M NaCl as described for the functional assay. Mapping of the particle surface using AFM reveals that the observed virus-like objects are removed from the material (Fig. 3C) and the smooth surface of the H-

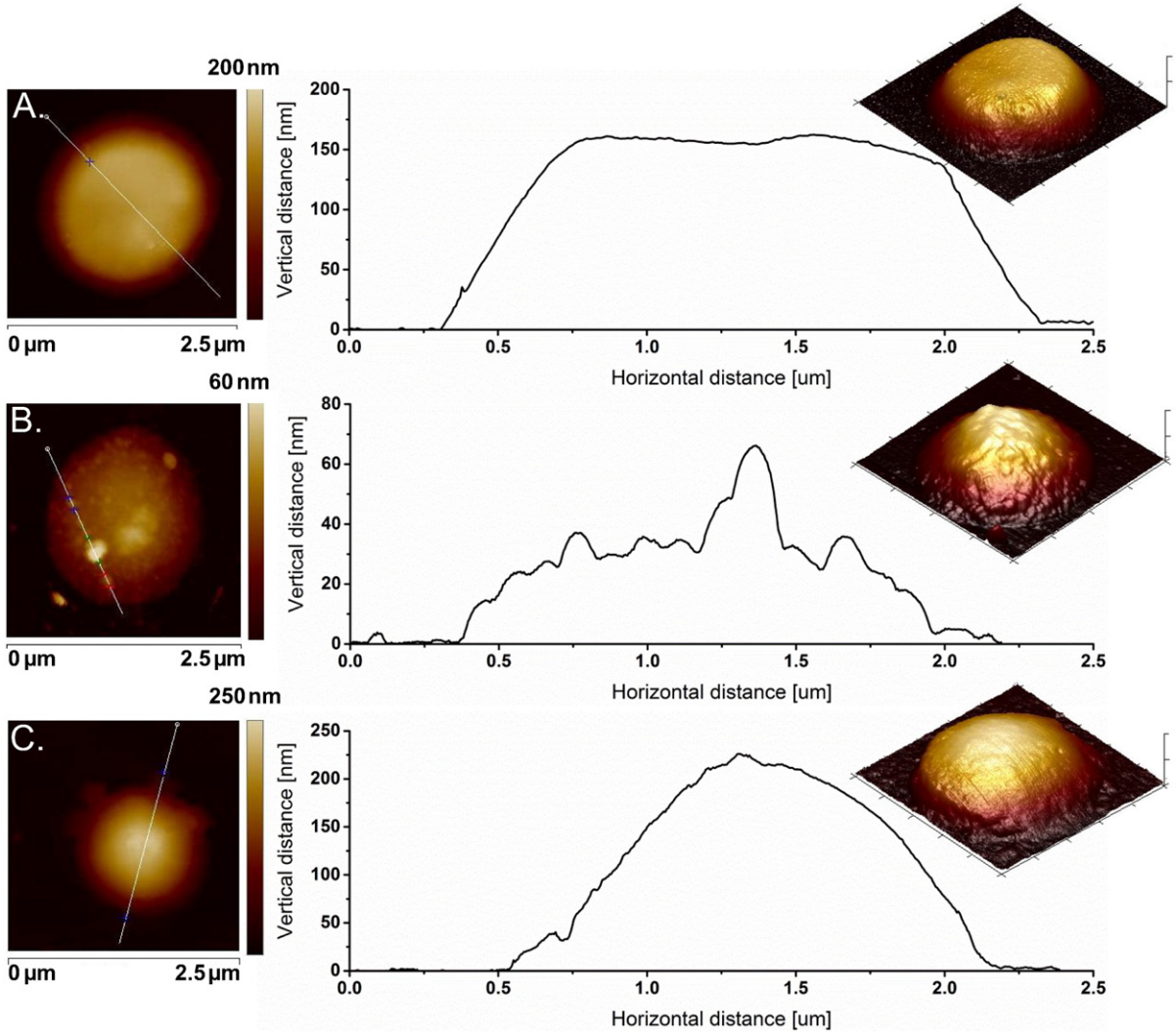

Fig. 3. H-HTCC NS/MS bind HCoV NL63 virions. Height, cross section and 3D AFM topography images of H-HTCC-MS incubated with lysate of mock infected (A) or virus infected (B) cells. H-HTCC-NS/MS imaged after desorption with 2 M NaCl (C). Scan size: 2.5 × 2.5 µm for 2D figures. Scan size and the vertical scale on 3D figures: 2.5 × 2.5 µm and 100 nm (A); 2.0 × 2.0 µm and 50 nm (B); and 1.0 × 1,0 µm and 100 nm (C), respectively.

HTCC-NS/MS is restored. Obtained results strongly suggest that HCoV-NL63 virions are adsorbed on the surface of H-HTCC-NS/MS, while no binding of cellular material was observed in the control sample, suggesting high selectivity.

3.4. Influence of the degree of cationization of HTCC-NS/MS on the efficiency of HCoV-NL63 adsorption and desorption

The virus desorption from the polymeric particles observed in the solutions with increased ionic strength implied that the virus adsorption/desorption may be also influenced by the degree of cationization of the particles surface. Therefore, the experiments were carried out using polymeric particles with low (L-HTCC-NS/MS), medium (M-HTCC-NS/MS) and high (H-HTCC-NS/MS) degree of surface modification and their properties were compared with those of the non-modified chitosan particles (CHIT-NS/MS). The number of adsorbed HCoV-NL63 particles present in the samples containing these materials was assessed using qRT-PCR. The results are presented in Fig. 4 were normalized and expressed in LRV (Log Removal Value) units which are widely used to express the efficiency of a process of water purification from bacteria and viruses [14,18,43,44]. LRV was calculated according to Eq. (1)

$$\mathrm{LRV} = \log_{10}\left(\frac{c_0}{c_i}\right) \quad (1)$$

where c_0 and c_i represent viral RNA yield (copies/milliliter) in the sample before and after adsorption, respectively.

The results indicate that the efficiency of HCoV-NL63 removal strongly depends on the degree of cationization of the adsorbent surface and is higher for more cationic HTCC-NS/MS. For 10 mg/500 μl of L-, M-, and H-HTCC-NS/MS the reduction in the number of HCoV-NL63 virions was 0.69, 2.44, and 3.1 LRV, respectively, which corresponded to the reduction by 79.58, 99.64, and 99.92%, respectively. The last number is very close to that of the "4-log rule" of EPA suggesting that water purification systems should attain the target efficiency of 99,99% for removal of viruses from drinking water [45]. The decrease in the number of HCoV-NL63 RNA copies after addition of 10 mg/500 μl CHIT-NS/MS was not statistically significant indicating that the CHIT-NS/MS surface has not high enough charge density to bind HCoV-NL63. Observed results are consistent with data reported previously [32].

3.5. Virus binding capacity of H-HTCC-NS/MS

After the adsorption and desorption of virions on the developed material was confirmed, an effort was made to assess the capacity of H-HTCC-NS/MS, as described in Section 2.8. Briefly, HCoV-NL63 was incubated with different amounts of H-HTCC-NS/MS and adsorbed infectious virus was recovered with 2 M NaCl. The amounts of recovered virus were evaluated by titration (Fig. 5).

It was found that the infectivity of HCoV-NL63 significantly decreased after incubation of the viral suspensions with H-HTCC-NS/MS due to the adsorption of viral particles on H-HTCC-NS/MS leading to a decrease in the number of infective free viral particles. This decrease in $TCID_{50}$ could be well correlated with the concentration of the adsorbent particles used. The presence of 2.5, 5.0 and 10 mg/500 μl H-HTCC-NS/MS in the viral samples resulted in a ~187-, ~415-, and ~700-fold decrease in $TCID_{50}$, respectively, corresponding to >99.4, 99.7, and 99.8% reduction in the virus titer, respectively.

To confirm the correlation between the amount of virus adsorbed and the concentration of the adsorbent the qRT-PCR analysis was applied (Fig. 6). An evident decrease in the number of copies of viral RNA was found in the viral suspensions after addition of H-HTCC-NS/MS. Furthermore, the decrease can be correlated with the amount of H-HTCC-NS/MS, e.g., for 2.5 mg/500 μl H-HTCC-NS/MS sample LRV is ~2.4 (i.e., 99.60% decrease), while for both 5- and 10 mg/500 μl of H-HTCC-NS/MS LRVs were ~3.1 (i.e., 99.92% decrease) (Fig. 6).

The viral particles were then desorbed by increasing the ionic strength of the solution with 2 M NaCl. As expected this resulted in the release of HCoV-NL63 from the surface of H-HTCC-NS/MS although the number of RNA copies released did not increase monotonically with increasing adsorbent concentration (data not shown).

3.6. Specificity of the adsorption of different coronaviruses

We previously found that the water-soluble HTCC is a strong inhibitor of HCoV-NL63 and mouse hepatitis virus (MHV) [31], however, it is a very weak inhibitor of human coronavirus HCoV-OC43 [32]. To find out if the virus inhibitory activity of HTCC is correlated with its adsorptive properties, we studied the specificity of the adsorption of these coronavirus strains by H-HTCC-NS/MS. For this purpose, monolayers of LR7 and HCT-8 cells were infected with MHV and HCoV-OC43, respectively. The infections were carried out for 2 (MHV) and 6 (HCoV-OC43) days at 37 °C and 32 °C, respectively. The virus titrations have shown that MHV titer decreases from $TCID_{50}$ of ~6,285,500 to ~250,200 (about 25 times) due to adsorption on 5 mg/500 μl H-HTCC-NS/MS while it did not significantly change for HCoV-OC43 (Fig. 7). Therefore, this polymeric material can be used also for the effective adsorption of MHV, another coronavirus inhibited by water soluble HTCC. It was thus found that the coronaviral strains inhibited by water-soluble HTCC are also adsorbed by the particles made of this polymer which confirms that the anticoronaviral activity of HTCC is due to its direct attractive interaction with the respective viruses.

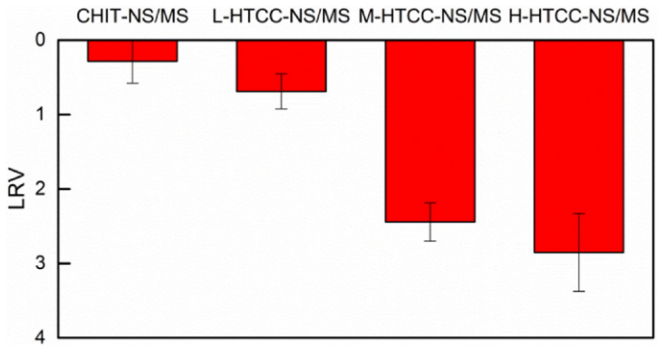

Fig. 4. The decrease in the number of HCoV-NL63 RNA copies in the virus suspension incubated with 10 mg/500 μl of CHIT-NS/MS, L-, M-, and H-HTCC NS/MS, as found from qRT-PCR. All experiments were repeated thrice and values are presented as an average ± SD.

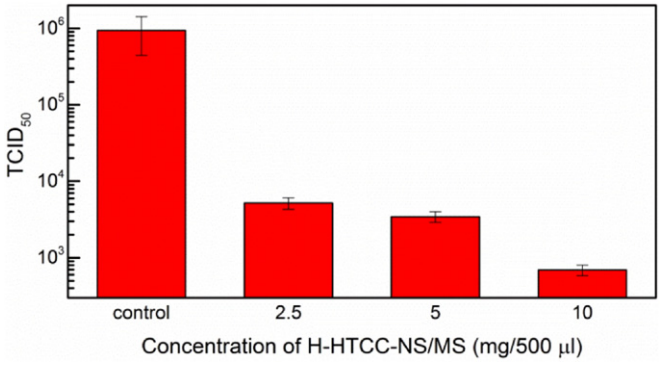

Fig. 5. Capacity of H-HTCC-NS/MS. HCoV-NL63 titers (50% tissue culture infective dose ($TCID_{50}$) per milliliter), in the virus sample which did not contain H-HTCC-NS/MS (control) and in the viral suspension incubated with 2.5, 5.0, and 10 mg/500 μl of H-HTCC-NS/MS. All experiments were repeated thrice and values are presented as an average ± SD.

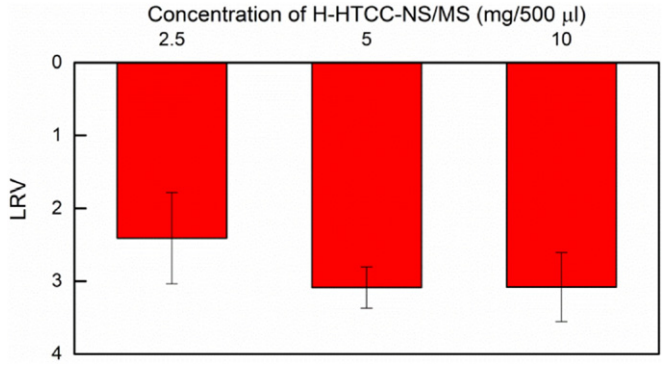

Fig. 6. The decrease in the number of HCoV-NL63 RNA copies in the virus suspension incubated with 2.5, 5 or 10 mg/500 µl of H-HTCC-NS/MS as found from qRT-PCR. All experiments were repeated thrice and values are presented as an average ± SD.

4. Conclusions

HTCC-NS/MS were obtained and used for adsorption of coronaviruses from aqueous suspensions. It was found that HCoV-NL63 and MHV can be adsorbed on the surface of HTCC-NS/MS, while no significant adsorption was observed in the case of human coronavirus OC43 (HCoV-OC43). Importantly, HCoV-NL63 is selectively adsorbed in the presence of lysed cell components which indicates that HTCC-NS/MS may be used for virus purification. The correlation of the adsorptive properties of HTCC particles with the virus inhibitory activity of its water-soluble form suggests that the nature of the inhibition is similar to that observed for neutralizing antibodies. Moreover, desorption of the HCoV-NL63 virions adsorbed on the HTCC-NS/MS surface is also possible by applying medium with high ionic strength. Noteworthy, desorbed HCoV-NL63 retained infectiousness. The increased degree of cationization of the polymeric particles enhanced adsorption of HCoV-NL63. This fact together with ionic strength-induced virus desorption indicate that the virus-polymer interaction is due to the electrostatic Coulomb attraction. Strong and selective adsorption of HCoV-NL63 combined with the possibility of the virus desorption with retained virulence indicate that HTCC-NS/MS is a material with a great potential in the detection, removal, separation, concentration and/or purification of HCoV-NL63 coronavirus.

Author contributions

The manuscript was written through contributions of all authors. JC contributed to the synthesis of materials, conducting biological studies, collection of data, analysis of results, and preparation of the manuscript. MN, KS and KP provided idea of the project, guidance and contributed to manuscript preparation. KW performed AFM analysis. All authors have read and given approval to the final version of the manuscript.

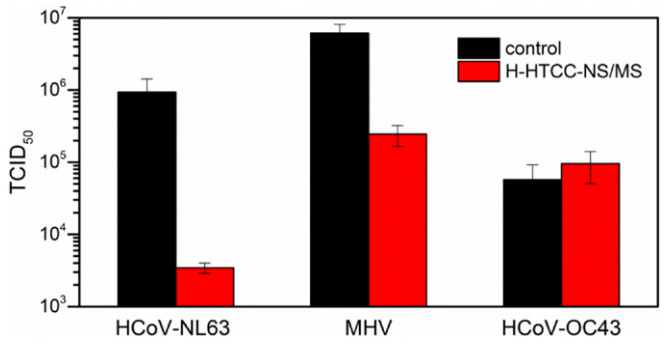

Fig. 7. TCID50 of HCoV-NL63 and MHV after incubation with 5 mg/500 µl H-HTCC-NS/MS. All experiments were repeated thrice and values are presented as an average ± SD.

Conflict of interest

All authors declare no conflicts of interests.

Acknowledgment

Foundation for Polish Science provided funding to JC under grant number VENTURES/2013-11/1 cofinanced by the EU European Regional Development Fund.

National Science Center, Poland, provided funding to Justyna Ciejka under grant number UMO-2016/21/D/ST5/01661.

National Centre for Research and Development, Poland, provided funding to KP under grant number Lider/27/55/L-2/10/2011.

National Science Center, Poland, provided funding to KP under grant number UMO-2012/07/E/NZ6/01712. KP acknowledges a networking contribution by the COST Action CM1407 ("Challenging organic syntheses inspired by nature - from natural products chemistry to drug discovery"). Parts of this research were carried out with equipment purchased thanks to the financial support of European Union structural funds (grants POIG.02.01.00-12-064/08 and POIG.02.01.00-12-167/08). The Faculty of Biochemistry, Biophysics and Biotechnology of the Jagiellonian University is a partner of the Leading National Research Center supported by the Ministry of Science and Higher Education of the Republic of Poland.

The funders had no role in study design, data collection and analysis, the decision to publish, or preparation of the manuscript.

Appendix A. Supplementary data

Details about the physicochemical characterization of the polymeric materials (i.e. FTIR-ATR spectra, DLS and elemental composition of the samples) can be found in the electronic supplementary information. This material is available free of charge via the Internet. Supplementary data associated with this article can be found in the online version, at http://dx.doi.org/10.1016/j.msec.2017.03.047

References

[1] T. Rodrigues, M.J.T. Carrondo, P.M. Alvesa, P.E. Cruz, Purification of retroviral vectors for clinical application: biological implications and technological challenges, J. Biotechnol. 127 (2007) 520–541.
[2] A. Ali, M.J. Roossinck, Rapid and efficient purification of Cowpea chlorotic mottle virus by sucrose cushion ultracentrifugation, J. Virol. Methods 141 (2007) 84–86.
[3] V. Baekelandt, K. Eggermont, M. Michiels, B. Nuttin, Z. Debyser, Optimized lentiviral vector production and purification procedure prevents immune response after transduction of mouse brain, Gene Ther. 10 (2003) 1933–1940.
[4] L. Tuschong, S.L. Soenen, R.M. Blaese, F. Candotti, L.M. Muul, Immune response to fetal calf serum by two adenosine deaminase-deficient patients after T cell gene therapy, Hum. Gene Ther. 13 (2002) 1605–1610.
[5] S.T. Andreadis, C.M. Roth, J.M. Le Doux, J.R. Morgan, M.L. Yarmush, Large-scale processing of recombinant retroviruses for gene therapy, Biotechnol. Prog. 15 (1999) 1–11.
[6] Z. Altintas, M. Gittens, J. Pocock, I.E. Tothill, Biosensors for waterborne viruses: detection and removal, Biochimie 115 (2015) 144–154.
[7] C. Charcosset, Membrane processes in biotechnology: an overview, Biotechnol. Adv. 24 (2006) 482–492.
[8] M. Nasimuzzaman, D. Lynn, R. Ernst, M. Beuerlein, R.H. Smith, A. Shrestha, S. Cross, K. Link, C. Lutzko, D. Nordling, D.W. Russell, A. Larochelle, P. Malik, J.C.M. Van Der Loo, Production and Purification of High-titer Foamy Virus Vector for the Treatment of Leukocyte Adhesion Deficiency, 2016 3.
[9] R.P. Araldi, D.N.S. Giovanni, T.C. Melo, N. Diniz, J. Mazzuchelli-de-Souza, T.A. Sant'Ana, R.F. Carvalho, W. Beçak, R.C. Stocco, Bovine papillomavirus isolation by ultracentrifugation, J. Virol. Methods 208 (2014) 119–124.
[10] L. Kremser, G. Bilek, D. Blaas, E. Kenndler, Capillary electrophoresis of viruses, subviral particles and virus complexes, J. Sep. Sci. 30 (2007) 1704–1713.
[11] L. Kremser, D. Blaas, E. Kenndler, Capillary electrophoresis of biological particles: viruses, bacteria, and eukaryotic cells, Electrophoresis 25 (2004) 2282–2291.
[12] A. Bonfá, R.S.N. Saito, R.F.O. França, B.A.L. Fonseca, D.F.S. Petri, Poly(ethylene glycol) decorated poly(methylmethacrylate) nanoparticles for protein adsorption, Mater. Sci. Eng. C 31 (2011) 562–566.
[13] M.D.L.M. Segura, A. Kamen, P. Trudel, A. Garnier, A novel purification strategy for retrovirus gene therapy vectors using heparin affinity chromatography, Biotechnol. Bioeng. 90 (2005) 391–404.

[14] T. Vicente, M.F.Q. Sousa, C. Peixoto, J.P.B. Mota, P.M. Alves, M.J.T. Carrondo, Anion-exchange membrane chromatography for purification of rotavirus-like particles, J. Membr. Sci. 311 (2008) 270–283.
[15] K.S. Zerda, C.P. Gerba, K.C. Hou, S.M. Goyal, Adsorption of viruses to charge-modified silica, Appl. Environ. Microbiol. 49 (1985) 91–95.
[16] J.A. Park, J.K. Kang, J.H. Kim, S.B. Kim, S. Yu, T.H. Kim, Bacteriophage removal in various clay minerals and clay-amended soils, Environ. Eng. Res. 20 (2015) 133–140.
[17] S. Chattopadhyay, R.W. Puls, Adsorption of bacteriophages on clay minerals, Environ. Sci. Technol. 33 (1999) 3609–3614.
[18] H. Ma, C. Burger, B.S. Hsiao, B. Chu, Ultra-fine cellulose nanofibers: new nano-scale materials for water purification, J. Mater. Chem. 21 (2011) 7507.
[19] K. Viswanathan, P. Rathish, V.P. Gopinath, R. Janice, Raj G. Dhinakar, In ovo delivery of Newcastle disease virus conjugated hybrid calcium phosphate nanoparticle and to study the cytokine profile induction, Mater. Sci. Eng. C (2014) 45.
[20] E. Imbert-Laurenceau, J. Crepinior, J.M. Crance, A. Jouan, V. Migonney, Polystyrene derivatives substituted with arginine interact with Babanki (Togaviridae) and Kedougou (Flaviviridae) viruses, J. Med. Virol. 69 (2003) 503–509.
[21] F. Ogura, K. Hayashi, J.-B. Lee, K. Kanekiyo, T. Hayashi, Evaluation of an edible blue-green alga, *Aphanothece sacrum*, for its inhibitory effect on replication of herpes simplex virus type 2 and influenza virus type a, Biosci. Biotechnol. Biochem. 74 (2010) 1687–1690.
[22] S. Preeprame, K. Hayashi, J.B. Lee, U. Sankawa, T. Hayashi, A novel antivirally active fucan sulfate derived from an edible brown alga, *Sargassum horneri*, Chem. Pharm. Bull. 49 (2001) 484–485.
[23] X. Mi, K.S. Vijayaragavan, C.L. Heldt, Virus adsorption of water-stable quaternized chitosan nanofibers, Carbohydr. Res. 387 (2014) 24–29.
[24] M.F. Tafur, K.S. Vijayaragavan, C.L. Heldt, Reduction of porcine parvovirus infectivity in the presence of protecting osmolytes, Antivir. Res. 99 (2013) 27–33.
[25] X. Li, P. Wu, G.F. Gao, S. Cheng, Carbohydrate-functionalized chitosan fiber for influenza virus capture, Biomacromolecules 12 (2011) 3962–3969.
[26] A. Lisov, V. Vrublevskaya, Z. Lisova, A. Leontievsky, O. Morenkov, A 2,5-dihydroxybenzoic acid-gelatin conjugate: the synthesis, antiviral activity and mechanism of antiviral action against two alphaherpesviruses, Viruses 7 (2015) 5343–5360.
[27] P.J. Budge, Y. Li, J.A. Beeler, B.S. Graham, RhoA-derived peptide dimers share mechanistic properties with other polyanionic inhibitors of respiratory syncytial virus (RSV), including disruption of viral attachment and dependence on RSV G, J. Virol. 78 (2004) 5015–5022.
[28] A. Karger, B. Bettin, H. Granzow, T.C. Mettenleiter, Simple and rapid purification of alphaherpesviruses by chromatography on a cation exchange membrane, J. Virol. Methods 70 (1998) 219–224.
[29] R.S. Moore, D.H. Taylor, L.S. Sturman, M.M. Reddy, G.W. Fuhs, Poliovirus adsorption by 34 minerals and soils, Appl. Environ. Microbiol. 42 (1981) 963–975.
[30] K. Clark, A. Sarr, P. Grant, T. Phillips, G. Woode, In vitro studies on the use of clay, clay minerals and charcoal to adsorb bovine rotavirus and bovine coronavirus, Vet. Microbiol. 63 (1998) 137–146.
[31] A. Milewska, J. Ciejka, K. Kaminski, A. Karewicz, D. Bielska, S. Zeglen, W. Karolak, M. Nowakowska, J. Potempa, B.J. Bosch, K. Pyrc, K. Szczubialka, Novel polymeric inhibitors of HCoV-NL63, Antivir. Res. 97 (2013) 112–121.
[32] A. Milewska, K. Kaminski, J. Ciejka, K. Kosowicz, S. Zeglen, J. Wojarski, M. Nowakowska, K. Szczubialka, K. Pyrc, HTCC: broad range inhibitor of coronavirus entry, PLoS One 11 (2016), e0156552.
[33] A. Milewska, M. Zarebski, P. Nowak, K. Stozek, J. Potempa, K. Pyrc, Human coronavirus NL63 utilizes heparan sulfate proteoglycans for attachment to target cells, J. Virol. 88 (2014) 13221–13230.
[34] Y. Chen, Y. Yang, Q. Liao, W. Yang, W. Ma, J. Zhao, X. Zheng, Y. Yang, R. Chen, Preparation, property of the complex of carboxymethyl chitosan grafted copolymer with iodine and application of it in cervical antibacterial biomembrane, Mater. Sci. Eng. C 67 (2016) 247–258.
[35] V. Nart, M.T. França, D. Anzilaggo, M.K. Riekes, J.M. Kratz, C.E.M. De Campos, C.M.O. Simões, H.K. Stulzer, Ball-milled solid dispersions of BCS class IV drugs: impact on the dissolution rate and intestinal permeability of acyclovir, Mater. Sci. Eng. C 53 (2015) 229–238.
[36] L. Li, J. Zhang, C. Li, L. Chen, R. Qiao, A facile method for synthesizing water-soluble and superior sustained release anti-HIV prodrug SCs-d4T, Mater. Sci. Eng. C 49 (2015) 84–92.
[37] K. Kamiński, K. Zazakowny, K. Szczubiałka, M. Nowakowska, pH-sensitive genipin-cross-linked chitosan microspheres for heparin removal, Biomacromolecules 9 (2008) 3127–3132.
[38] L.J. Reed, H. Muench, A simple method of estimating fifty per cent endpoints, Am. J. Epidemiol. 27 (1938) 493–497.
[39] K. Kamiński, K. Szczubiałka, K. Zazakowny, R. Lach, M. Nowakowska, Chitosan derivatives as novel potential heparin reversal agents, J. Med. Chem. 53 (2010) 4141–4147.
[40] I. Lynch, K.A. Dawson, Protein-nanoparticle interactions, Nano Today 3 (2008) 40–47.
[41] A. Armanious, M. Aeppli, R. Jacak, D. Refardt, T. Sigstam, T. Kohn, M. Sander, Viruses at solid-water interfaces: a systematic assessment of interactions driving adsorption, Environ. Sci. Technol. 50 (2016) 732–743.
[42] Y. Lin, X. Yan, W. Cao, C. Wang, J. Feng, J. Duan, S. Xie, Short communication probing the structure of the SARS coronavirus using, Antivir. Ther. 9 (2004) 287–289.
[43] B.V. Bhut, J. Weaver, A.R. Carter, S.R. Wickramasinghe, S.M. Husson, The role of polymer nanolayer architecture on the separation performance of anion-exchange membrane adsorbers: part II. DNA and virus separations, Biotechnol. Bioeng. 108 (2011) 2654–2660.
[44] B. Michen, J. Fritsch, C. Aneziris, T. Graule, Improved virus removal in ceramic depth filters modified with MgO, Environ. Sci. Technol. 47 (2013) 1526–1533.
[45] US EPA, Ground Water Rule, October 2006.